Elastic properties of graphene

M. I. Katsnelson
P. Le Doussal
B. Horowitz
K. Wiese
J. Gonzalez
P. San-Jose
V. Parente
B. Amorim
R. Roldan
C. Gomez-Navarro
J. Gomez
G. Lopez-Polin
F. Perez-Murano
A. Morpurgo
N. J. G. Couto
C. Stampfer

Correlations, criticality, and coherence in quantum systems
Évora, Portugal, 6-10 October 2014

Outline

- The stiffness of graphene
- Defects and elastic constants
- Electronic transport and corrugations

GRAPHENE'S SUPERLATIVES

- Thinnest imaginable material
- largest surface area (~2,700 m^2 per gram)
- strongest material 'ever measured' (theoretical limit)
- stiffest known material (stiffer than diamond)
- most stretchable crystal (up to 20% elastically)
- record thermal conductivity (outperforming diamond)
- highest current density at room T (106 times of copper)
- completely impermeable (even He atoms cannot squeeze through)
- highest intrinsic mobility (100 times more than in Si)
- conducts electricity in the limit of no electrons
- lightest charge carriers (zero rest mass)
- longest mean free path at room T (micron range)

Why are there two dimensional crystals?

STATISTICAL PHYSICS

by

L. D. LANDAU AND E. M. LIFSHITZ

INSTITUTE OF PHYSICAL PROBLEMS,
U.S.S.R. ACADEMY OF SCIENCES

Volume 5 of *Course of Theoretical Physics*

PART 1
THIRD EDITION, REVISED AND ENLARGED
by E. M. LIFSHITZ and L. P. PITAEVSKII

ered). It is easy to see, however, that the thermal fluctuations "smooth out" such a crystal, so that ϱ = constant is the only possibility: the mean

Thermal fluctuations:

$$\langle \vec{u}(L)\vec{u}(0)\rangle \approx \frac{k_B T}{B}\log\left(\frac{L}{d}\right)$$

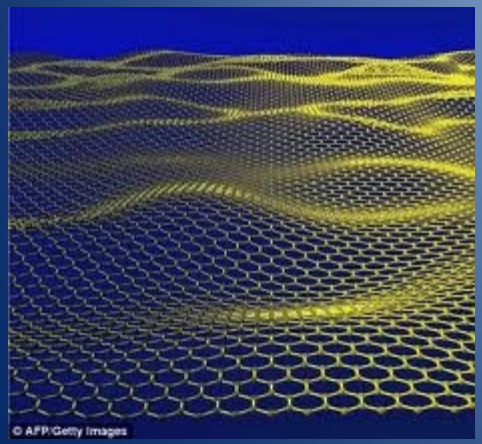

$B_{graphene}$ =22 eV Å^{-2} = 352 N/m

$B_{diamond}$ x d=52.4 N/m

T=300K

L=1Km

$\langle \vec{u}(L)\vec{u}(0)\rangle \approx 0.03\text{Å}^2$

Elastic properties of graphene

Measurement of the Elastic Properties and Intrinsic Strength of Monolayer Graphene

Changgu Lee,[1,2] Xiaoding Wei,[1] Jeffrey W. Kysar,[1,3] James Hone[1,2,4]*

We measured the elastic properties and intrinsic breaking strength of free-standing monolayer graphene membranes by nanoindentation in an atomic force microscope. The force-displacement behavior is interpreted within a framework of nonlinear elastic stress-strain response, and yields second- and third-order elastic stiffnesses of 340 newtons per meter (N m^{-1}) and −690 N m^{-1}, respectively. The breaking strength is 42 N m^{-1} and represents the intrinsic strength of a defect-free sheet. These quantities correspond to a Young's modulus of E = 1.0 terapascals, third-order elastic stiffness of D = −2.0 terapascals, and intrinsic strength of σ_{int} = 130 gigapascals for bulk graphite. These experiments establish graphene as the strongest material ever measured, and show that atomically perfect nanoscale materials can be mechanically tested to deformations well beyond the linear regime.

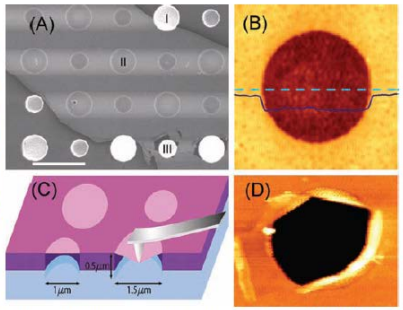

Fig. 1. Images of suspended graphene membranes. **(A)** Scanning electron micrograph of a large graphene flake spanning an array of circular holes 1 μm and 1.5 μm in diameter. Area I shows a hole partially covered by graphene, area II is fully covered, and area III is fractured from indentation. Scale bar, 3 μm. **(B)** Noncontact mode AFM image of one membrane, 1.5 μm in diameter. The solid blue line is a height profile along the dashed line. The step height at the edge of the membrane is about 2.5 nm. **(C)** Schematic of nanoindentation on suspended graphene membrane. **(D)** AFM image of a fractured membrane.

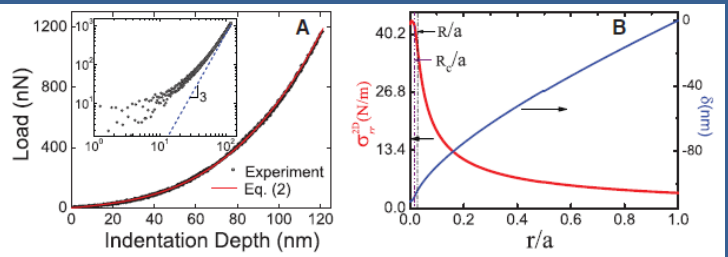

Fig. 2. **(A)** Loading/unloading curve and curve fitting to Eq. 2. The curve approaches cubic behavior at high loads (inset). **(B)** Maximum stress and deflection of graphene membrane versus normalized radial distance at maximum loading (simulation based on nonlinear elastic behavior in Eq. 1). The dashed lines indicate the tip radius R and contact radius R_c.

KUNGL. VETENSKAPS-AKADEMIEN
THE ROYAL SWEDISH ACADEMY OF SCIENCES

OCTOBER 5, 2010

Appendix, some properties of graphene

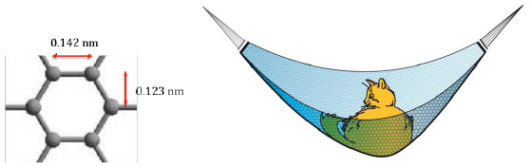

CLAIM #1: GRAPHENE CAN HOLD AN ELEPHANT

"…graphene as the strongest material ever measured, some 200 times stronger than structural steel. … If a sheet of cling film (which typically has a thickness of around 100 μm) were to have the same strength as pristine graphene, it would require a force of over 20,000 N to puncture it with a pencil,"."

Jim Hone, Columbia U

physicsworld.com

Graphic: Sci. Am., 11/2011

courtesy of M. M. Fogler

VOLUME 69, NUMBER 8 PHYSICAL REVIEW LETTERS 24 AUGUST 1992

Self-Consistent Theory of Polymerized Membranes

Pierre Le Doussal [a]
Institute for Advanced Study, Princeton, New Jersey 08540

Leo Radzihovsky
Lyman Laboratory, Harvard University, Cambridge, Massachusetts 02138
(Received 18 May 1992)

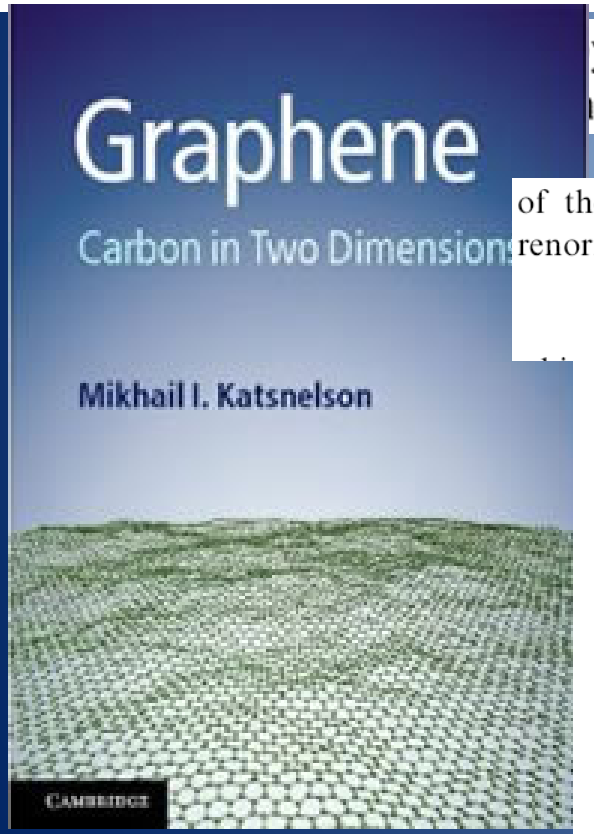

y a nontrivial fixed point, but with *anomalous*
stants $\lambda(q) \sim \mu(q) \sim q^{\eta_u}$, $\eta_u > 0$, with η_u

of the order of a^{-1} to make A dimensionless. One can assume also a renormalization of effective Lamé constants:

$$\lambda_R(q),\ \mu_R(q) \sim q^{\eta_u}, \qquad (9.103)$$

PHYSICAL REVIEW B **82**, 125435 (2010)

Self-consistent screening approximation for flexible membranes: Application to graphene

K. V. Zakharchenko, R. Roldán, A. Fasolino, and M. I. Katsnelson
Institute for Molecules and Materials, Radboud University Nijmegen, Heyendaalseweg 135, 6525 AJ Nijmegen, The Netherlands
(Received 9 June 2010; revised manuscript received 20 August 2010; published 20 September 2010)

Crystalline membranes at finite temperatures have an anomalous behavior of the bending rigidity that makes them more rigid in the long-wavelength limit. This issue is particularly relevant for applications of graphene in nanoelectromechanical and microelectromechanical systems. We calculate numerically the height-height correlation function $G(q)$ of crystalline two-dimensional membranes, determining the renormalized bending rigidity, in the range of wave vectors q from 10^{-7} Å^{-1} till 10 Å^{-1} in the self-consistent screening approximation (SCSA). For parameters appropriate to graphene, the calculated correlation function agrees reasonably with the results of atomistic Monte Carlo simulations for this material within the range of q from 10^{-2} Å^{-1} till 1 Å^{-1}. In the limit $q \to 0$ our data for the exponent η of the renormalized bending rigidity $\kappa_R(q) \propto q^{-\eta}$ is compatible with the previously known analytical results for the SCSA $\eta \simeq 0.82$. However, this limit appears to be reached only for $q < 10^{-5}$ Å^{-1} whereas at intermediate q the behavior of $G(q)$ cannot be described by a single exponent.

Experiments

C. Gomez-Navarro, J. Gomez, G. Lopez-Polin, F. Perez-Murano

Measurement of the Elastic Properties and Intrinsic Strength of Monolayer Graphene

Changgu Lee,[1,2] Xiaoding Wei,[1] Jeffrey W. Kysar,[1,3] James Hone[1,2,4]*

We measured the elastic properties and intrinsic breaking strength of free-standing monolayer graphene membranes by nanoindentation in an atomic force microscope. The force-displacement behavior is interpreted within a framework of nonlinear elastic stress-strain response, and yields second- and third-order elasti
respectively. The breaking stre
defect-free sheet. These quant
third-order elastic stiffness of
for bulk graphite. These experi
and show that atomically perf
well beyond the linear regime

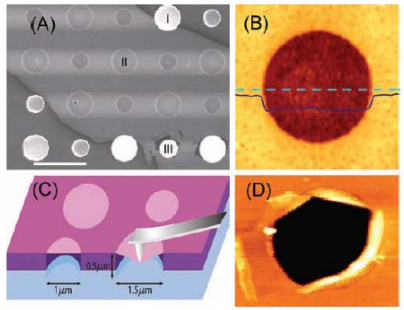

Fig. 1. Images of suspended graphene membranes. **(A)** Scanning electron micrograph of a large graphene flake spanning an array of circular holes 1 μm and 1.5 μm in diameter. Area I shows a hole partially covered by graphene, area II is fully covered, and area III is fractured from indentation. Scale bar, 3 μm. **(B)** Noncontact mode AFM image of one membrane, 1.5 μm in diameter. The solid blue line is a height profile along the dashed line. The step height at the edge of the membrane is about 2.5 nm. **(C)** Schematic of nanoindentation on suspended graphene membrane. **(D)** AFM image of a fractured membrane.

Experiments

Stiffening graphene by controlled defect creation

Authors: Guillermo López-Polín[1], Cristina Gómez-Navarro[1,2*], Vincenzo Parente[3], Francisco Guinea[3], Mikhail I. Katsnelson[4], Francesc Pérez-Murano[5], and Julio Gómez-Herrero[1,2]

arXiv:1406.2131

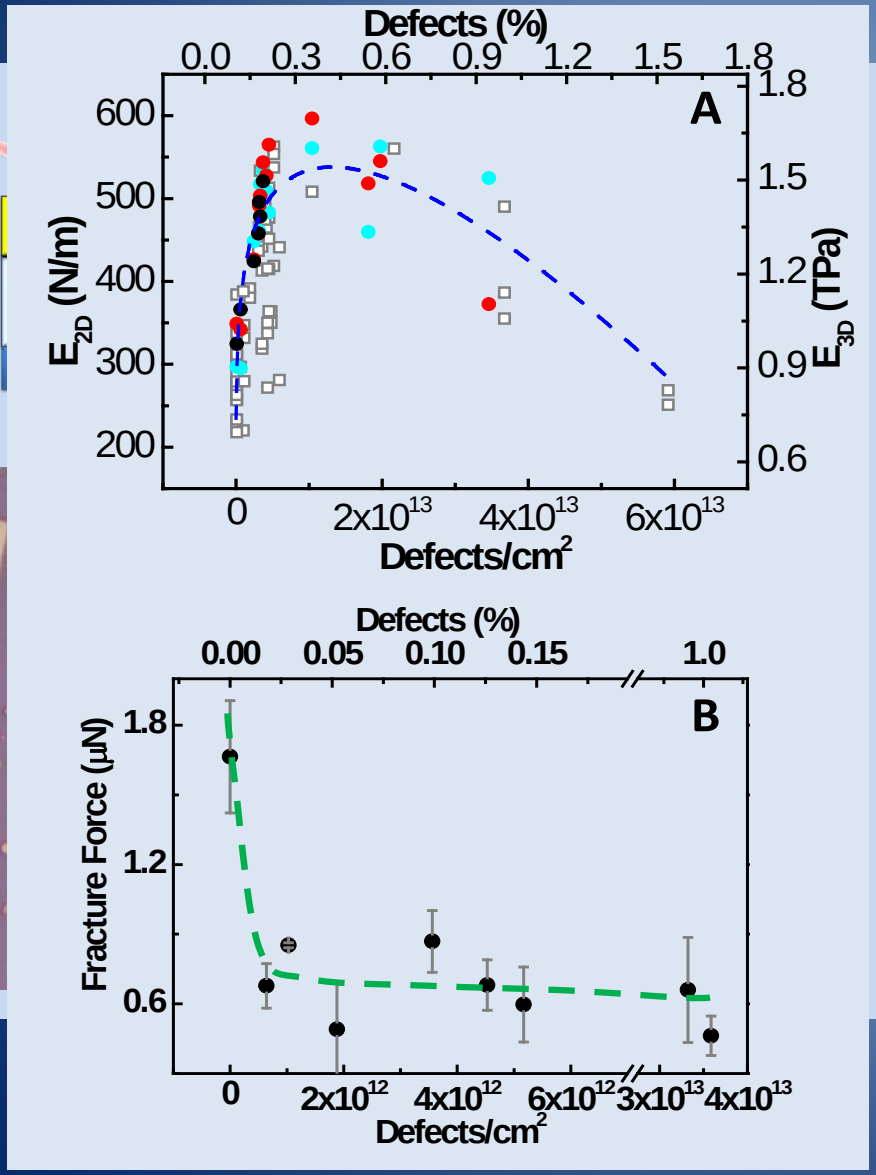

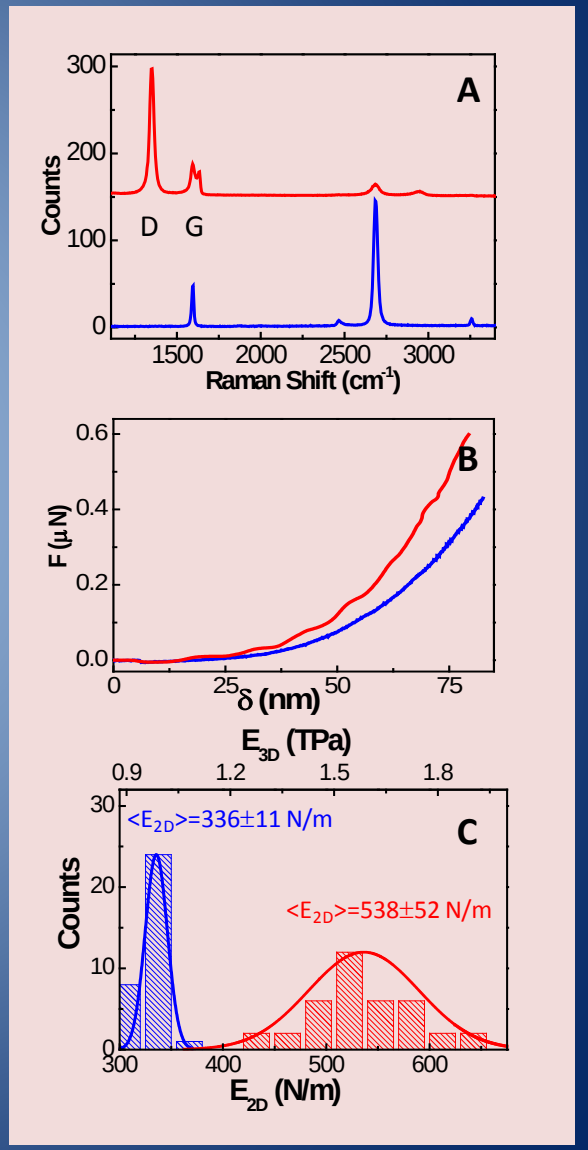

Two dimensional membranes

THEORY OF ELASTICITY

by

L. D. LANDAU AND E. M. LIFSHITZ

INSTITUTE OF PHYSICAL PROBLEMS, U.S.S.R. ACADEMY OF SCIENCES

Volume 7 of *Course of Theoretical Physics*

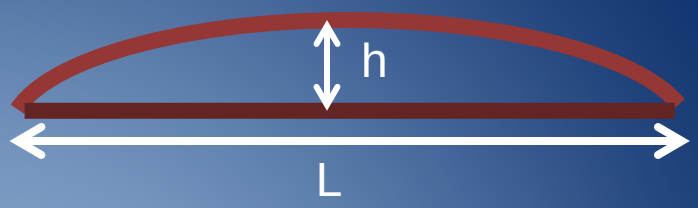

$$\Delta L \approx \frac{h^2}{2L}$$

Out of plane displacements lead to changes in area

Kinetic Bending Stretching

$$H = \frac{\rho}{2}\int d^2\vec{r}\,\frac{\partial^2 h}{\partial t^2} + \frac{\kappa}{2}\int d^2\vec{r}\left(\nabla^2 h\right)^2 + \frac{\lambda}{2}\int d^2\vec{r}\left(\partial_x u_x + \partial_y u_y + \frac{(\partial_x h)^2}{2} + \frac{(\partial_y h)^2}{2}\right)^2 +$$

$$+ \mu\int d^2\vec{r}\left[\left(\partial_x u_x + \frac{(\partial_x h)^2}{2}\right)^2 + \left(\partial_y u_y + \frac{(\partial_y h)^2}{2}\right)^2 + \frac{1}{2}\left(\partial_x u_y + \partial_y u_x + \frac{(\partial_x h)(\partial_y h)}{2}\right)^2\right]$$

Shear

Two dimensional crystaline membranes are intrinsically anharmonic

Thermal expansion

PHYSICAL REVIEW B **86**, 144103 (2012)

Bending modes, anharmonic effects, and thermal expansion coefficient in single-layer and multilayer graphene

In plane st

F

Gri

Th

$\alpha \approx$

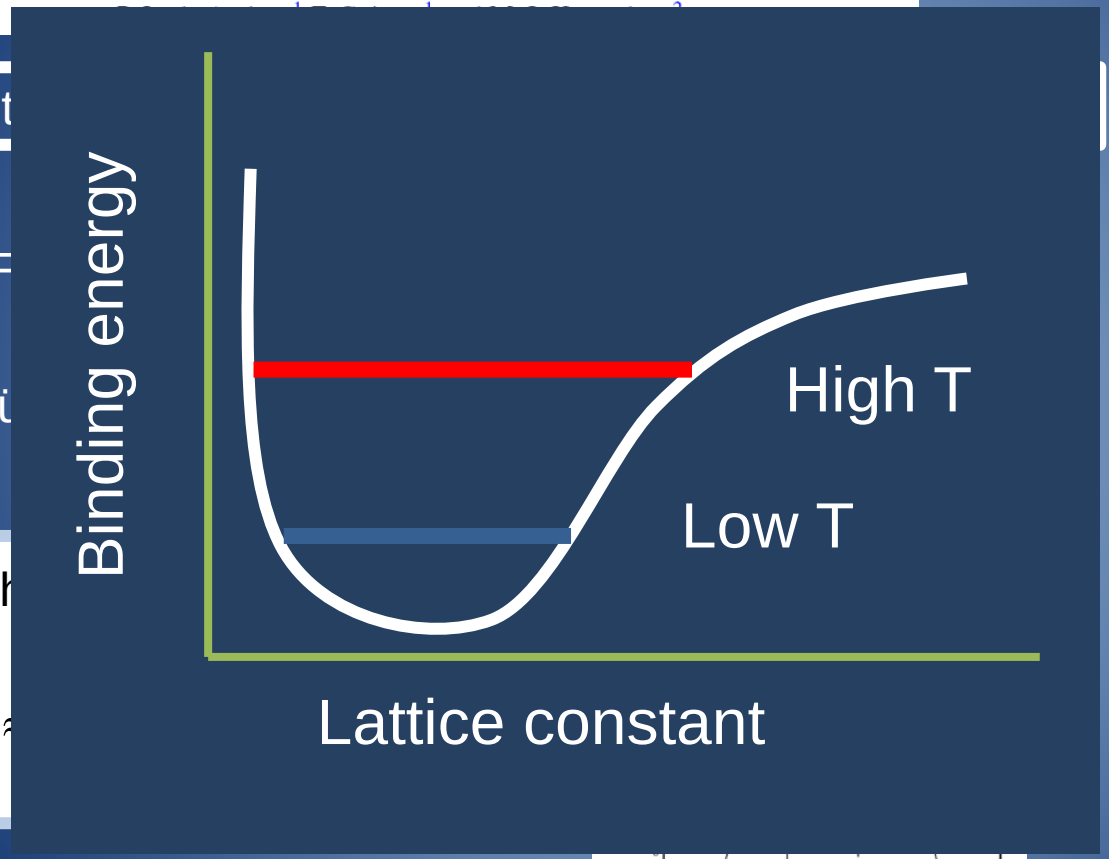

Negative thermal expansion coefficient

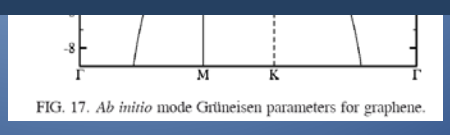

FIG. 17. *Ab initio* mode Grüneisen parameters for graphene.

PHYSICAL REVIEW B **71**, 205214 (2005)

First-principles determination of the structural, vibrational and thermodynamic properties of diamond, graphite, and derivatives

Nicolas Mounet* and Nicola Marzari†

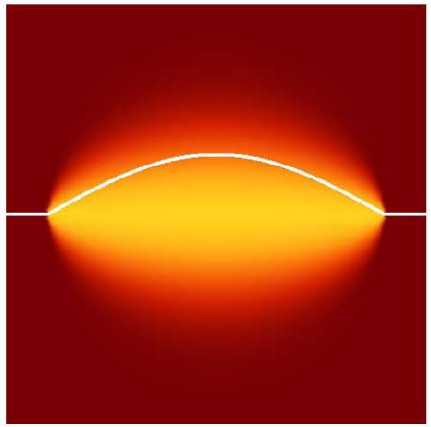

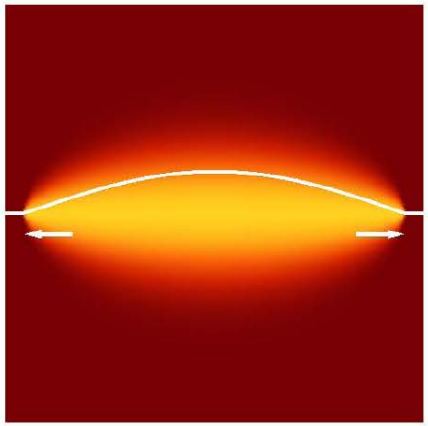

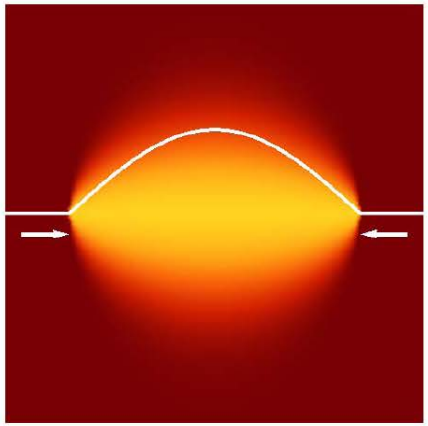

Substrate effects

PHYSICAL REVIEW B **88**, 115418 (2013)

Flexural mode of graphene on a substrate

Bruno Amorim* and Francisco Guinea

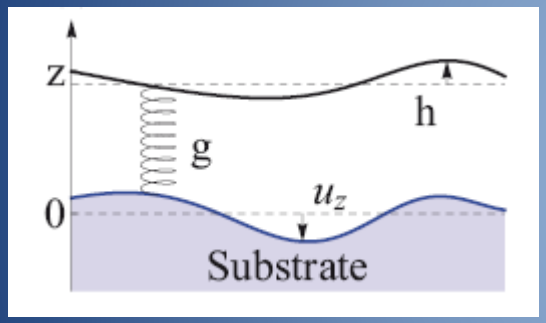

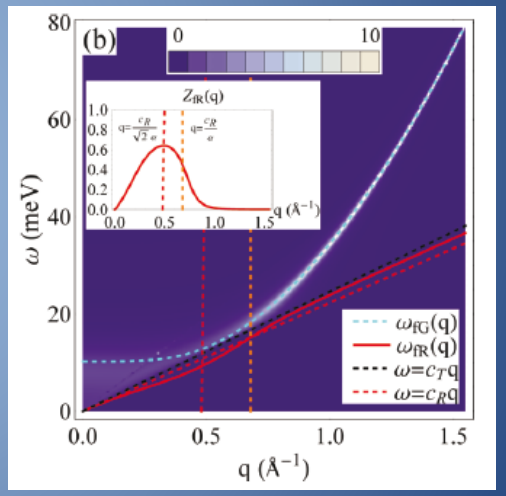

Gapped flexural modes

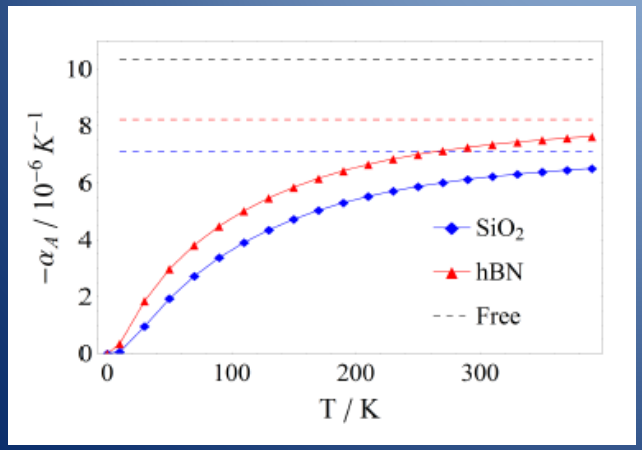

Thermal expansion

Out of plane fluctuations screen the in plane elastic constants

$$E \approx \left(c_1 Y \bar{u} + c_2 \frac{\kappa}{\ell^2} \right) h^2$$

$$F \approx T \log \left(\frac{T}{c_1 Y \bar{u} + c_2 \frac{\kappa}{\ell^2}} \right)$$

$$\delta Y = \frac{1}{\ell^2} \frac{\partial^2 F}{\partial \bar{u}^2} \propto -\frac{Y^2 T \ell^2}{\kappa^2}$$

$Y \approx 10\text{eV}\text{Å}^{-2}$

$T \approx 300\text{K} \approx 0.025\text{eV}$

$\kappa \approx 1\text{eV}$

$\ell \approx 10\text{Å}$

$\frac{Y T \ell^2}{\kappa^2} \approx 25 \gg 1$

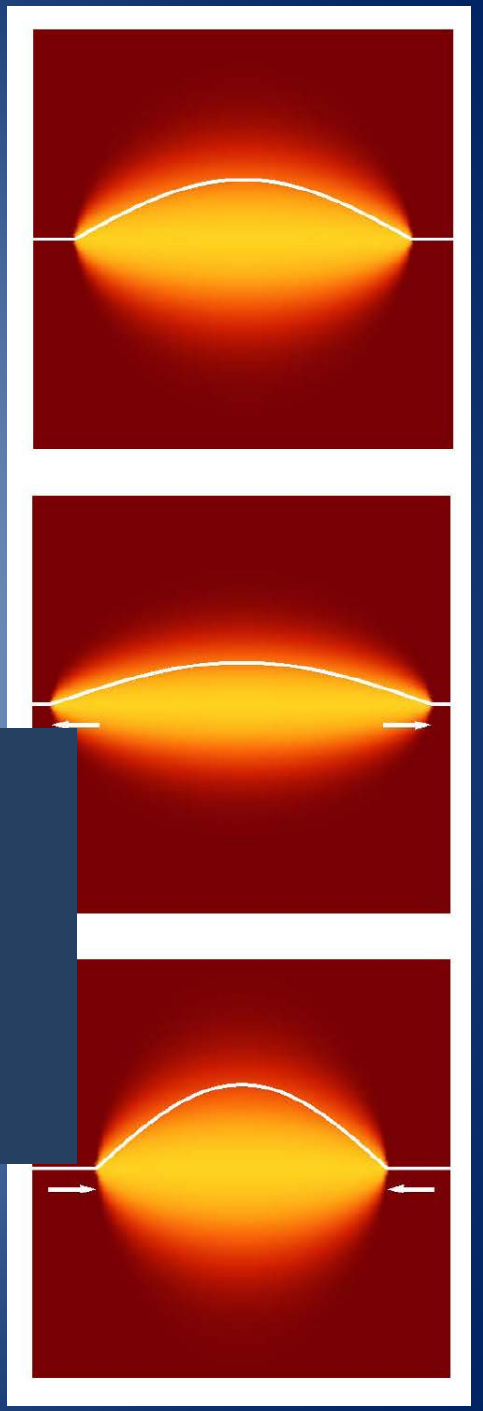

Numerical results

NANO LETTERS
Letter
pubs.acs.org/NanoLett

Acoustic Phonon Lifetimes and Thermal Transport in Free-Standing and Strained Graphene

Nicola Bonini,*,† Jivtesh Garg,‡ and Nicola Marzari§

PHYSICAL REVIEW B **87**, 214303 (2013)

Anharmonic properties from a generalized third-order *ab initio* approach: Theory and applications to graphite and graphene

Lorenzo Paulatto,* Francesco Mauri, and Michele Lazzeri

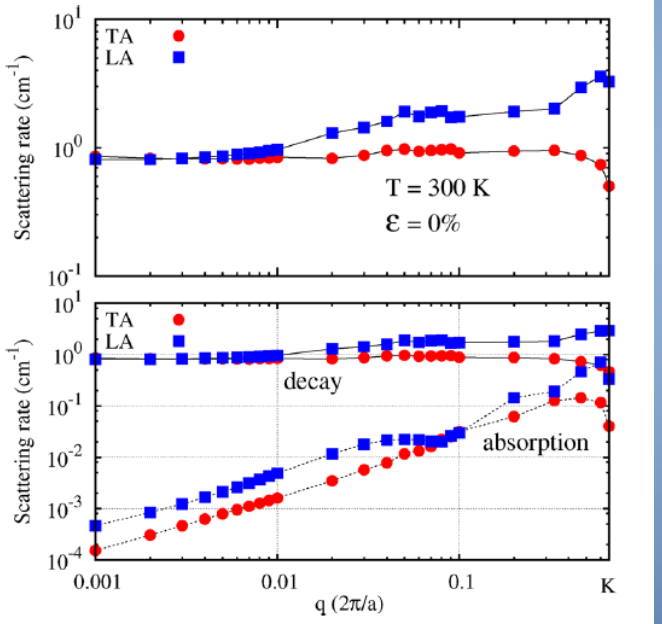

Figure 1. Upper panel: scattering rates for LA and TA modes alon the Γ–*K* direction in unstrained free-standing graphene at 300 K Lower panel: Contributions to the scattering rates due to decay (soli lines) and absorption (dashed line) processes.

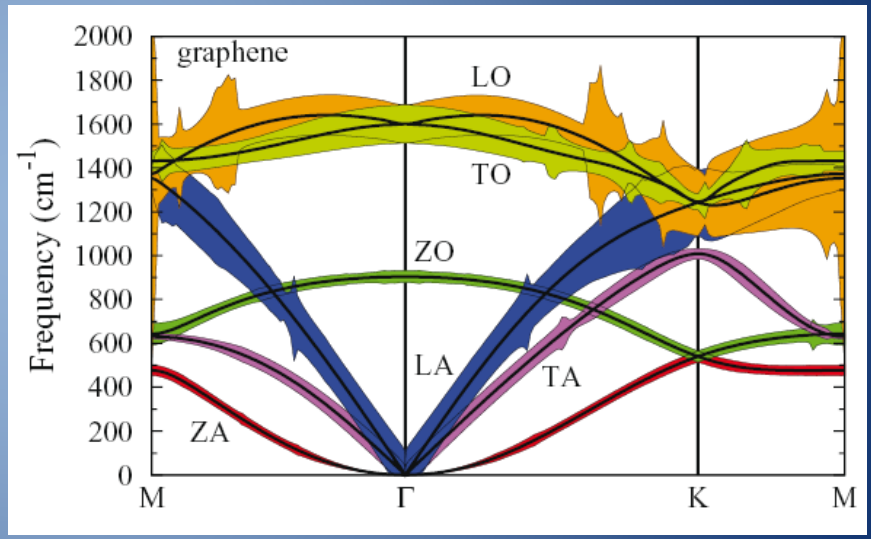

$$\Gamma_L = \frac{(\lambda+\mu)^2 T}{4(\lambda+2\mu)\kappa^{3/2}\rho^{1/2}}$$

$$\Gamma_T = \frac{\mu T}{4\kappa^{3/2}\rho^{1/2}}$$

Theory of elasticity

The self consistent screening approximation

Fluctuations in membranes with crystalline and hexatic order

D. R. Nelson and L. Peliti (*)

J. Physique, **48**, 1085 (1987)

$$\delta\kappa \propto \int d^2\vec{q}\,\frac{TY}{\kappa|\vec{q}|^4}$$

VOLUME 69, NUMBER 8 PHYSICAL REVIEW LETTERS 24 AUGUST 1992

Self-Consistent Theory of Polymerized Membranes

Pierre Le Doussal [a]
Institute for Advanced Study, Princeton, New Jersey 08540
Leo Radzihovsky
Lyman Laboratory, Harvard University, Cambridge, Massachusetts 02138

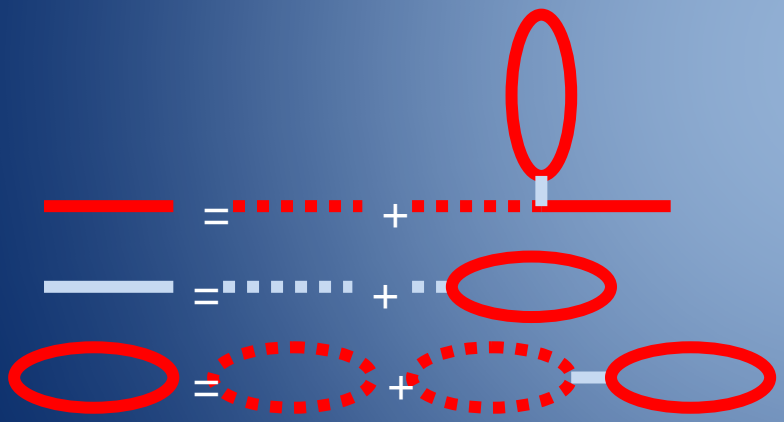

$$G^{-1}(\vec{q}) = G_0^{-1}(\vec{q}) - \Sigma(\vec{q})$$

$$\Sigma(\vec{q}) = \frac{2}{(2\pi)^2}\int d^2\vec{q}\,b(\vec{q})|\vec{q}P_T(\vec{p})\vec{q}|^2 G(\vec{q}-\vec{p})$$

$$b(\vec{q}) = \frac{b_0}{1+3b_0 I(\vec{q})}$$

$$I(\vec{p}) = \frac{1}{8(2\pi)^2}\int d^2\vec{q}\,|\vec{q}|^2|\vec{p}-\vec{q}|^2 G(\vec{q})G(\vec{p}-\vec{q})$$

$$\kappa(q) \propto q^{-\eta}$$

$$\lambda(q), \mu(q) \propto q^{\eta_u}$$

$$\eta \approx 0.821$$

$$\eta_u \approx 0.358$$

Power law divergences
Self consistent theory, valid in high dimensions
Agrees well with numerical simulaions

Vacancies and flexural modes

$$G(q,\omega)=\frac{1}{\rho\omega^2-\kappa q^4-\Sigma(q,\omega)}$$

T-matrix approximation

$$\Sigma(\omega)\approx\begin{cases} n_V\sqrt{\kappa\rho\omega^2} & h^2=0 \\ n_V\dfrac{\sqrt{\kappa\rho\omega^2}}{\log\left(\dfrac{\kappa}{a^4\rho\omega^2}\right)} & |\nabla h|^2=0 \end{cases}$$

infinite mass

vacancies

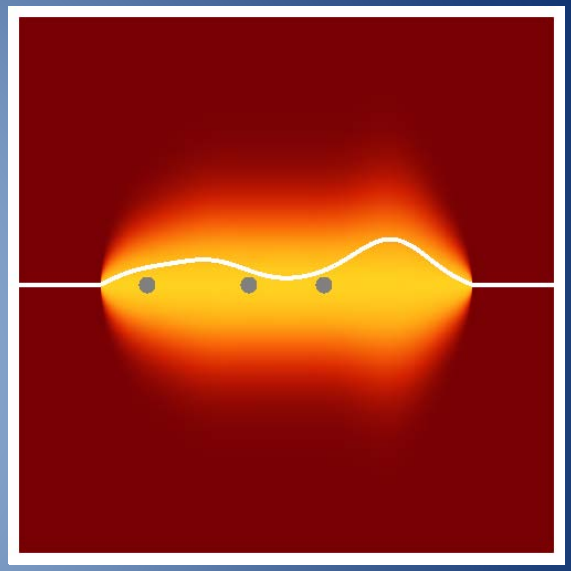

localization length

$$\frac{\kappa}{\ell^4}\approx\Sigma\left(\sqrt{\frac{\kappa}{\rho\ell^4}}\right)$$

$$\ell\approx n_V^{-1/2}$$

- Vacancies localize flexural modes
- Long wavelength flexural modes do not contribute to the screening of the elastic constants

geometric factor

percolation

$$Y \approx K\left(\frac{1}{R^2}+\frac{1}{\ell_0^2}+n_V\right)^{\frac{\eta_u}{2}}\left[1-c\left(\frac{1}{\ell_0^2}+n_V\right)\right]$$

intrinsic localization length

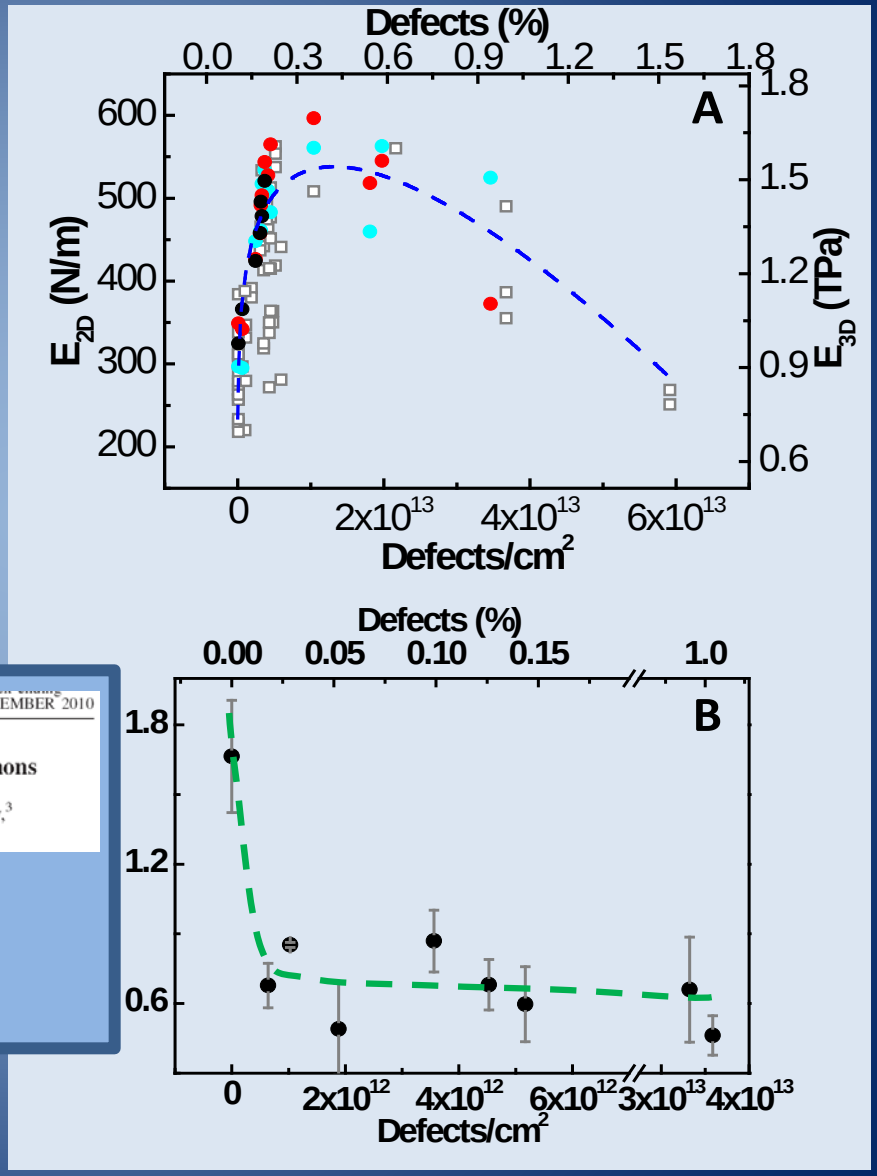

PRL 105, 266601 (2010) PHYSICAL REVIEW LETTERS 31 DECEMBER 2010

Limits on Charge Carrier Mobility in Suspended Graphene due to Flexural Phonons

Eduardo V. Castro,[1] H. Ochoa,[1] M. I. Katsnelson,[2] R. V. Gorbachev,[3] D. C. Elias,[3] K. S. Novoselov,[3] A. K. Geim,[3] and F. Guinea[1]

$$\ell_0 \approx 20-100\text{nm}$$

$$\ell_0 \geq k_F^{-1}$$

Young modulus and induced strains

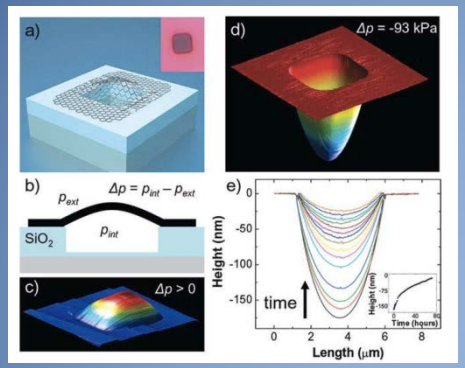

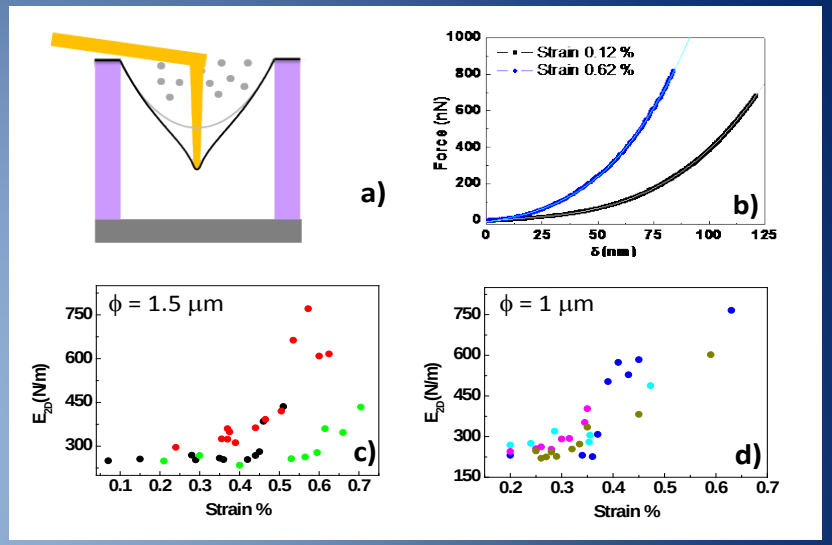

Experiments

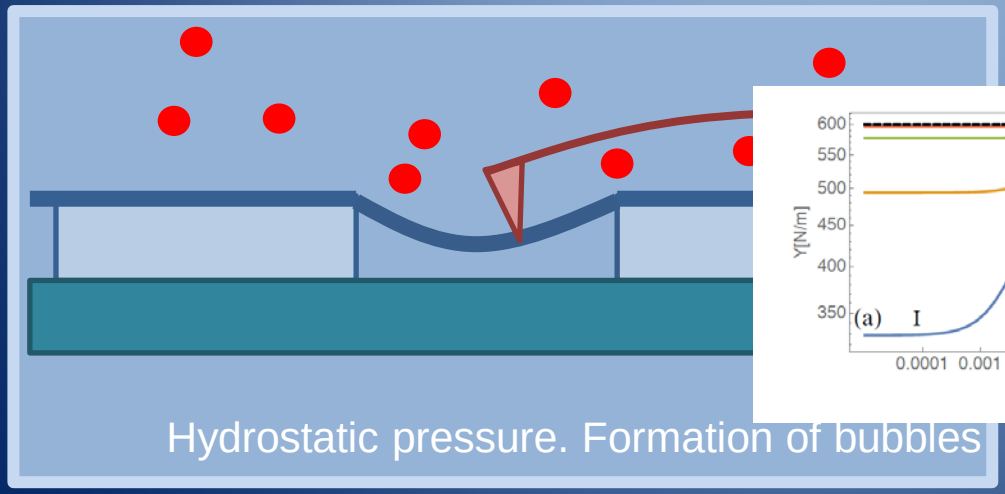

Hydrostatic pressure. Formation of bubbles

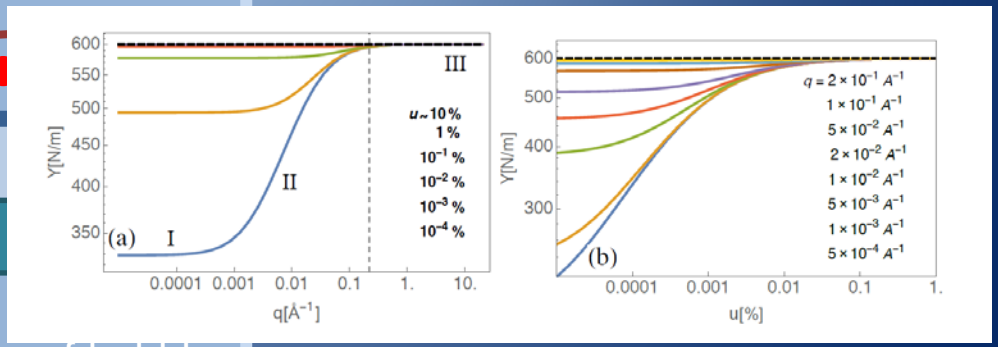

Theory

Graphene thermal expansion coefficient

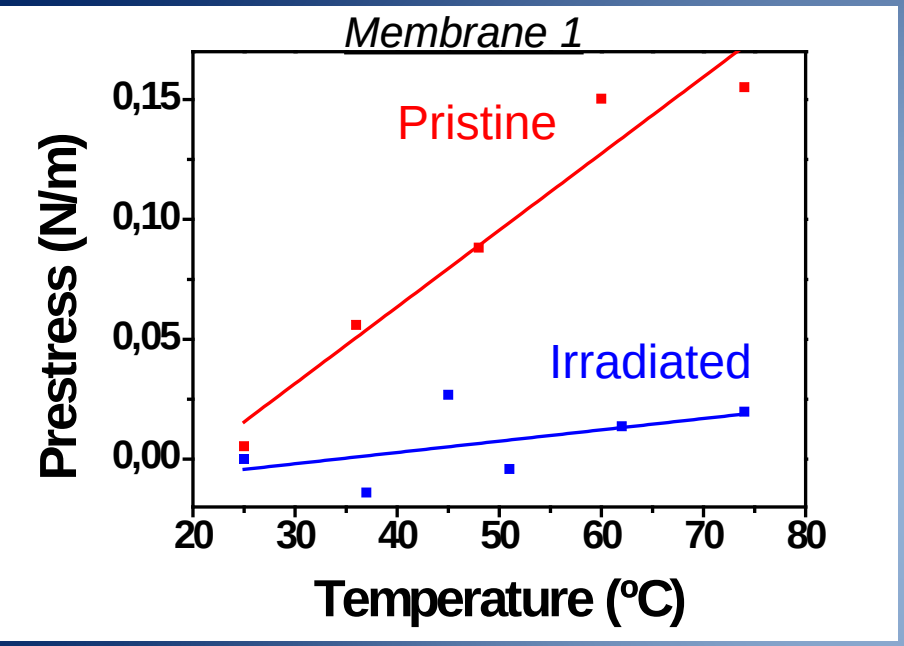

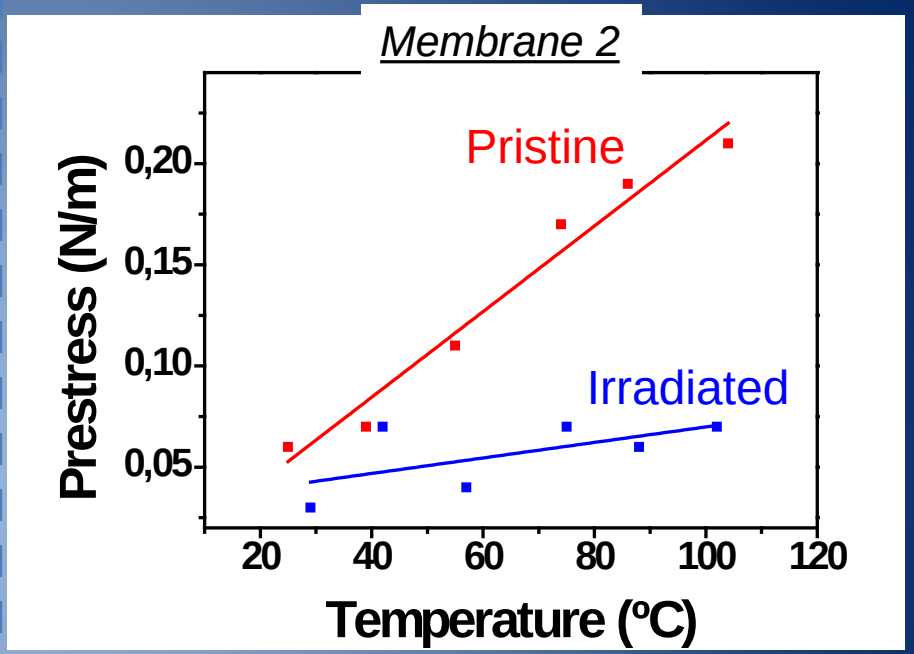

Thermal Expansion Coefficient:

- Pristine: $-9.4 \times 10^{-6}\ K^{-1}$
- Irradiated (L_D ~ 5.5 nm): $-1 \times 10^{-6}\ K^{-1}$

Thermal Expansion Coefficient:

- Pristine: $-6.2 \times 10^{-6}\ K^{-1}$
- Irradiated (L_D ~ 5 nm): $-1.1 \times 10^{-6}\ K^{-1}$

L_D : Mean distance between defects as measured by Raman

Electron-phonon coupling

Ripples induced by electrons

PRL 106, 045502 (2011) PHYSICAL REVIEW LETTERS week ending 28 JANUARY 2011

Electron-Induced Rippling in Graphene

P. San-Jose,[1] J. González,[1] and F. Guinea[2]

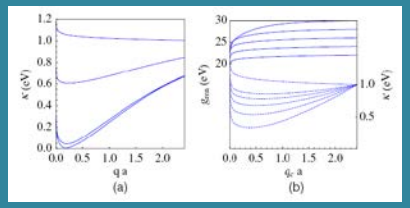

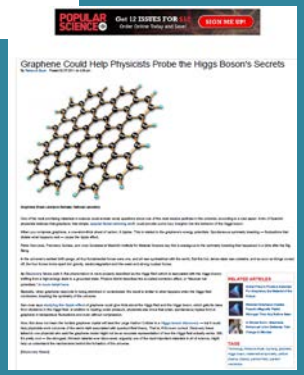

Quite remarkably, Eq. (13) exactly reproduces the structure of the effective potential for a relativistic scalar field theory in 3 + 1 dimensions [21]. This means that our model actually follows the same mechanism of symmetry breaking characteristic of a Higgs field in particle physics.

PHYSICAL REVIEW B 89, 125428 (2014)

Collective excitations in a large-*d* model for graphene

Francisco Guinea,[1] Pierre Le Doussal,[2] and Kay Jörg Wiese[2]

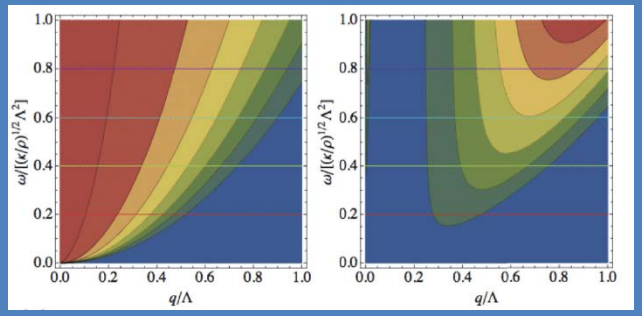

PHYSICAL REVIEW B 85, 201405(R) (2012)

Electron-hole puddles in the absence of charged impurities

Marco Gibertini,[1] Andrea Tomadin,[1] Francisco Guinea,[2] Mikhail I. Katsnelson,[3] and Marco Polini[1,*]

Charge puddles induced by strains

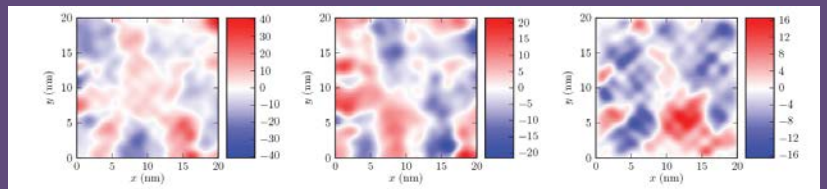

FIG. 2. (Color online) Left: Color/grayscale plot of the scalar potential $V_1(\boldsymbol{r})$ (in units of meV) calculated using Eq. (4) with $g_1 = 3$ eV. Center: The $\hat{x}$-component $A_x(\boldsymbol{r})$ of the vector potential (in units of meV) calculated using Eq. (4). Right: Same as in the central panel but for the $\hat{y}$-component $A_y(\boldsymbol{r})$ of the vector potential.

GRAPHENE'S SUPERLATIVES

- Thinnest imaginable material
- largest surface area (~2,700 m^2 per gram)
- strongest material 'ever measured' (theoretical limit)
- stiffest known material (stiffer than diamond)
- most stretchable crystal (up to 20% elastically)
- record thermal conductivity (outperforming diamond)
- highest current density at room T (106 times of copper)
- completely impermeable (even He atoms cannot squeeze through)
- highest intrinsic mobility (100 times more than in Si)
- conducts electricity in the limit of no electrons
- lightest charge carriers (zero rest mass)
- longest mean free path at room T (micron range)

Strains and conductivity in graphene

Random strain fluctuations as dominant disorder source for high-quality on-substrate graphene devices

Nuno J. G. Couto,[1] Davide Costanzo,[1] Stephan Engels,[2] Dong-Keun Ki,[1] Kenji Watanabe,[3] Takashi Taniguchi,[3] Christoph Stampfer,[4] Francisco Guinea,[5] and Alberto F. Morpurgo[1]

ArXiv:1401.5356, Phys. Rev. X, in press

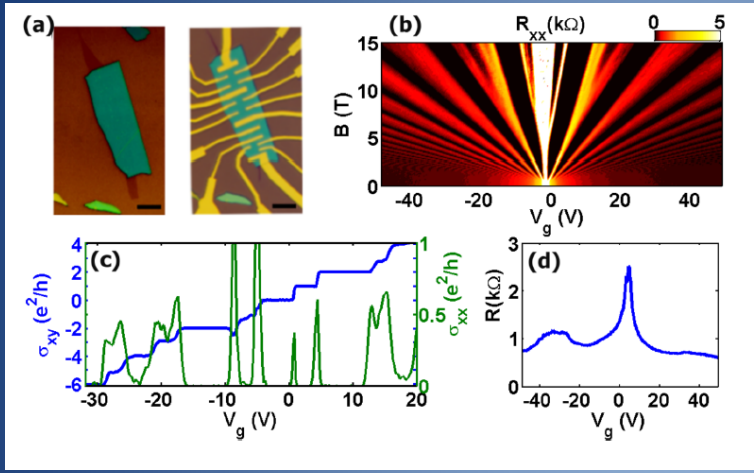

DC transport on graphene on BN
High mobility samples
Multiterminal devices

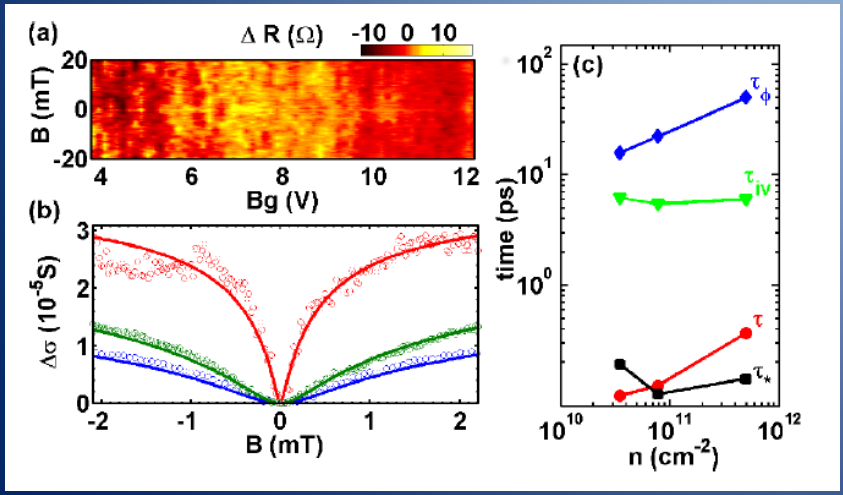

Magnetoresistance:
Scattering due to intravalley processes

Puddles and mobility

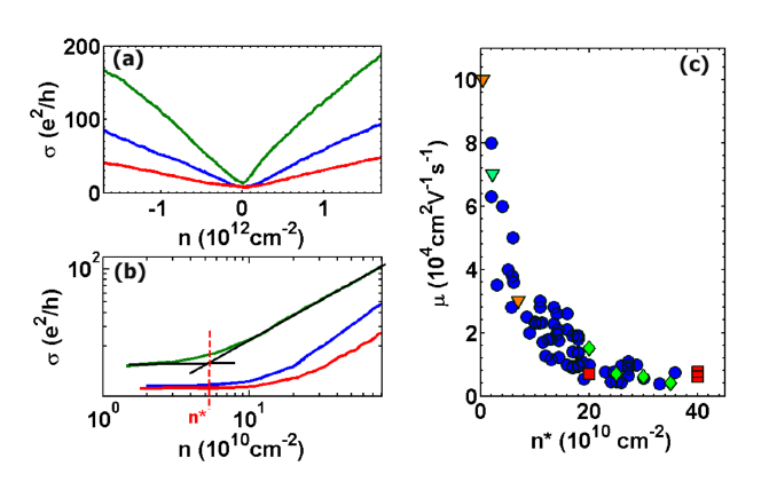

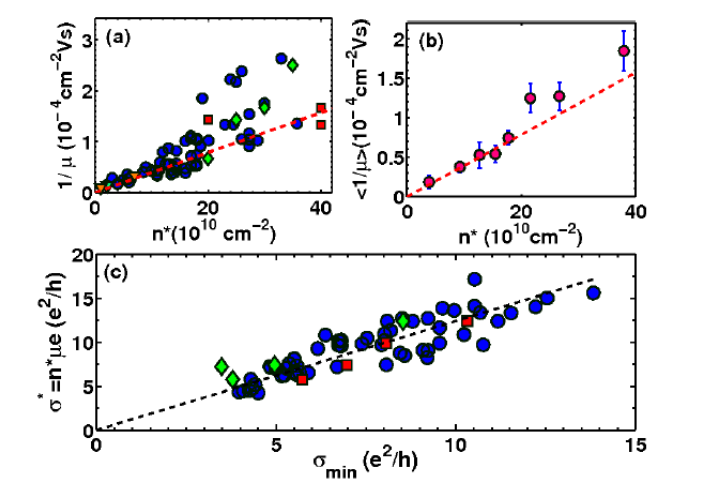

Mobility vs puddle density
Correlation independent of sample characteristics

- DC transport: mobility (roughly) independent of carrier concentration
- DC transport: correlation between mobility and puddles
- Weak localization: long range scatterers

Long range scattering mechanisms:
- Coulomb impurities
- Strains

Strains induce scalar and vector potentials

$$V_s(\vec{q}) = g_1 \frac{\mu_L}{\lambda_L + 2\mu_L}\left[u_{xx}(\vec{q}) + u_{yy}(\vec{q})\right]$$

$$\vec{A}_x(\vec{q}) = g_2 \frac{\lambda_L + \mu_L}{\lambda_L + 2\mu_L}\left[u_{xx}(\vec{q}) - u_{yy}(\vec{q})\right]$$

$$\vec{A}_y(\vec{q}) = 2g_2 \frac{\lambda_L + \mu_L}{\lambda_L + 2\mu_L} u_{xy}(\vec{q})$$

PHILOSOPHICAL TRANSACTIONS OF THE ROYAL SOCIETY A

Phil. Trans. R. Soc. A (2008) **366**, 195–204
doi:10.1098/rsta.2007.2157
Published online 19 November 2007

Electron scattering on microscopic corrugations in graphene

By M. I. Katsnelson[1,*] and A. K. Geim[2]

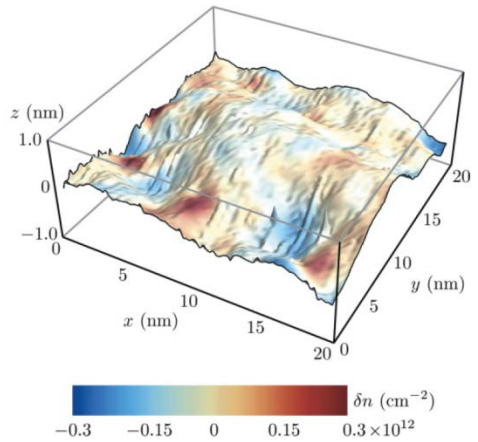

FIG. 1. (Color online) Three-dimensional plot of the corrugated graphene sample studied in this work [experimental data are a courtesy of Geringer (Ref. 20)]. The color/grayscale coding of the surface labels the local value of the induced carrier density $\delta n(\boldsymbol{r})$ as calculated from the Kohn-Sham-Dirac self-consistent theory, Eqs. (5)–(9). The data in this figure have been obtained by setting $g_1 = 3$ eV, $\alpha_{ee} = 0.9$, and $\bar{n}_c \approx 2.5 \times 10^{11}$ cm^{-2} (see text).

PHYSICAL REVIEW B **85**, 201405(R) (2012)

Electron-hole puddles in the absence of charged impurities

Marco Gibertini,[1] Andrea Tomadin,[1] Francisco Guinea,[2] Mikhail I. Katsnelson,[3] and Marco Polini

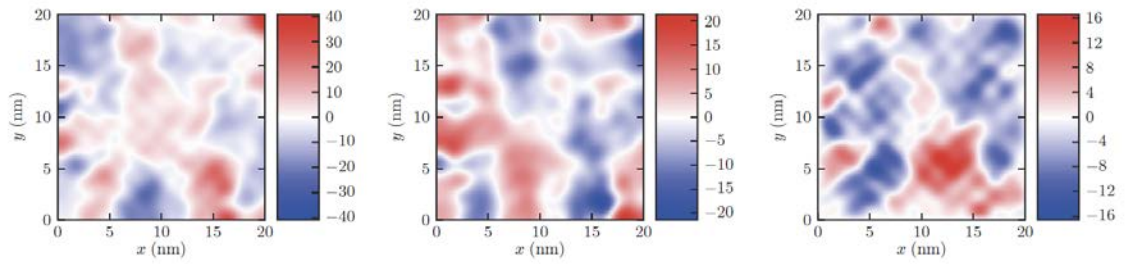

FIG. 2. (Color online) Left: Color/grayscale plot of the scalar potential $V_1(\boldsymbol{r})$ (in units of meV) calculated using Eq. (4) with $g_1 = 3$ eV. Center: The $\hat{x}$-component $A_x(\boldsymbol{r})$ of the vector potential (in units of meV) calculated using Eq. (4). Right: Same as in the central panel but for the $\hat{y}$-component $A_y(\boldsymbol{r})$ of the vector potential.

Relaxation times, mobilities, and puddles

$$\mu = \frac{\sigma}{ne} = 2\frac{e^2}{h}\frac{v_F k_F \tau}{ne}$$

$$\tau^{-1} = \tau_s^{-1} + \tau_g^{-1}$$

$$\tau_s^{-1} \approx \frac{2\pi}{\hbar^2}\frac{N(\epsilon_F)}{4\pi^2} \times \int_0^{\pi} d\theta \frac{1-\cos^2(\theta)}{2}\frac{\langle V_s(\vec{q})V_s(-\vec{q})\rangle}{\epsilon(\vec{q})^2}\Big|_{|\vec{q}|=2k_F\sin^2(\theta/2)}$$

$$\tau_g^{-1} \approx \frac{2\pi}{\hbar^2}\frac{N(\epsilon_F)}{4\pi^2} \times \int_0^{\pi} d\theta [1-\cos(\theta)]\langle \vec{A}_{\perp}(\vec{q})\vec{A}_{\perp}(-\vec{q})\rangle\Big|_{|\vec{q}|=2k_F\sin^2(\theta/2)}$$

$$n^*(\vec{r}) \approx \frac{1}{\pi}\left[\frac{V(\vec{r})}{\hbar v_F}\right]^2 \qquad \bar{n}^* = \frac{\langle V(\vec{r})^2\rangle}{\pi\hbar^2 v_F^2} = \frac{1}{4\pi^3\hbar^2 v_F^2}\int d^2\vec{q}\,\frac{\langle V_s(\vec{q})V_s(-\vec{q})\rangle}{\epsilon^2(\vec{q})}$$

Wrinkles and transport

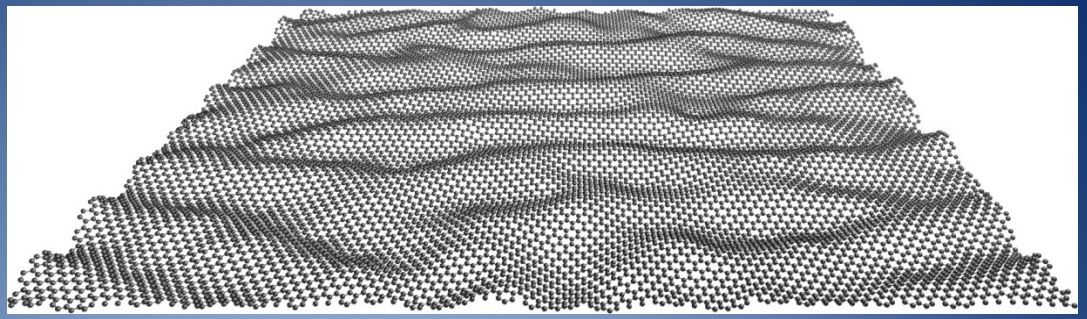

$$V_s(\vec{\mathbf{q}}) = -g_1 \frac{\mu_L}{\lambda_L + 2\mu_L} \frac{q_x^2 + q_y^2}{|\vec{\mathbf{q}}|^2} \mathcal{F}(\vec{\mathbf{q}})$$

$$A_x(\vec{\mathbf{q}}) = g_2 \frac{\lambda_L + \mu_L}{\lambda_L + 2\mu_L} \frac{q_x^2 - q_y^2}{|\vec{\mathbf{q}}|^2} \mathcal{F}(\vec{\mathbf{q}})$$

$$A_y(\vec{\mathbf{q}}) = -2g_2 \frac{\lambda_L + \mu_L}{\lambda_L + 2\mu_L} \frac{q_x q_y}{|\vec{\mathbf{q}}|^2} \mathcal{F}(\vec{\mathbf{q}})$$

Corrugations induce scalar and gauge potentials

Strains:

- Supress either weak localization, or weak antilocalization.
- Lead to long range, intravalley scattering.
- Induce puddles near the neutrality point.

$$\tau^{-1} = \tau_s^{-1} + \tau_g^{-1}$$

$$\tau_s^{-1} = \frac{2\pi}{\hbar^2} \frac{N(E_F)}{4\pi^2} \int_0^{\pi} d\theta \frac{[1-\cos^2(\theta)]}{2} \frac{\langle V_s(\vec{\mathbf{q}}) V_s(-\vec{\mathbf{q}})\rangle}{\epsilon^2(\vec{\mathbf{q}})}\Big|_{|\vec{\mathbf{q}}|=2k_F \sin(\theta/2)}$$

$$\tau_g^{-1} = \frac{2\pi}{\hbar^2} \frac{N(E_F)}{4\pi^2} \int_0^{\pi} d\theta \, [1-\cos(\theta)] \langle \vec{\mathbf{A}}_\perp(\vec{\mathbf{q}}) \vec{\mathbf{A}}_\perp(-\vec{\mathbf{q}})\rangle\Big|_{|\vec{\mathbf{q}}|=2k_F \sin(\theta/2)}$$

$$n^* = \frac{\langle V_s^2(\vec{\mathbf{r}})\rangle}{\pi\hbar^2 v_F^2} = \frac{1}{4\pi^3\hbar^2 v_F^2} \int d^2\vec{\mathbf{q}} \frac{\langle V_s(\vec{\mathbf{q}}) V_s(-\vec{\mathbf{q}})\rangle}{\epsilon^2(\vec{\mathbf{q}})}$$

$$\frac{1}{\mu n^*} \approx \frac{h}{e}\left[\frac{\pi(\hbar v_F)^2}{16e^4} + \frac{\pi g_2^2(\lambda_L+\mu_L)^2}{2g_1^2\mu_L^2}\right] \log^{-1}\left(\frac{\Lambda}{k_F^*}\right)$$

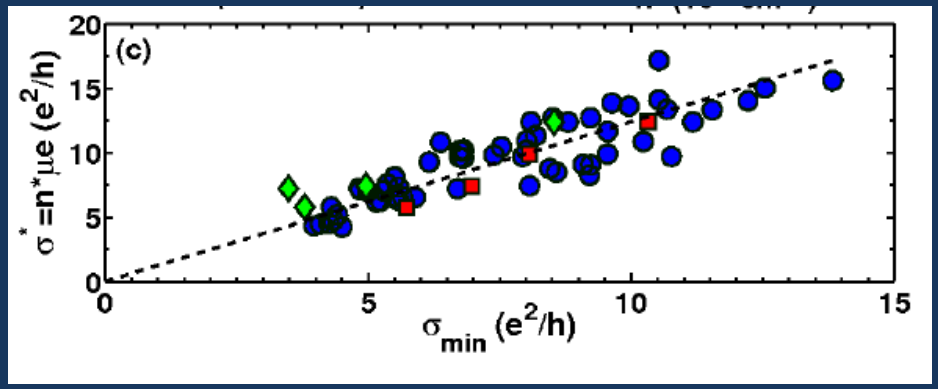

Substrate induced random forces

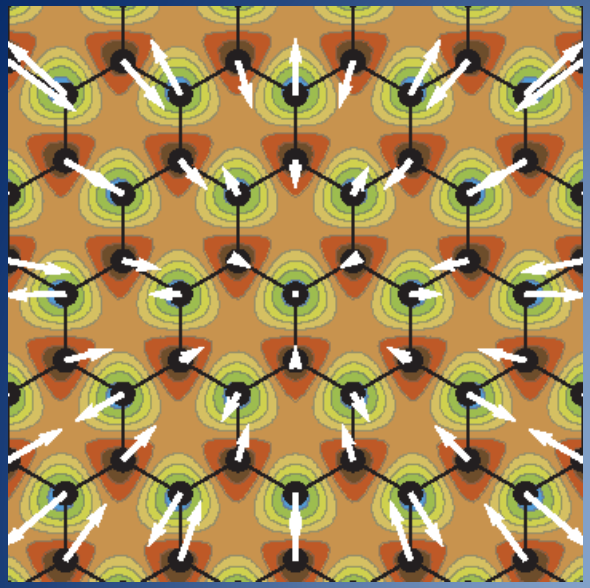

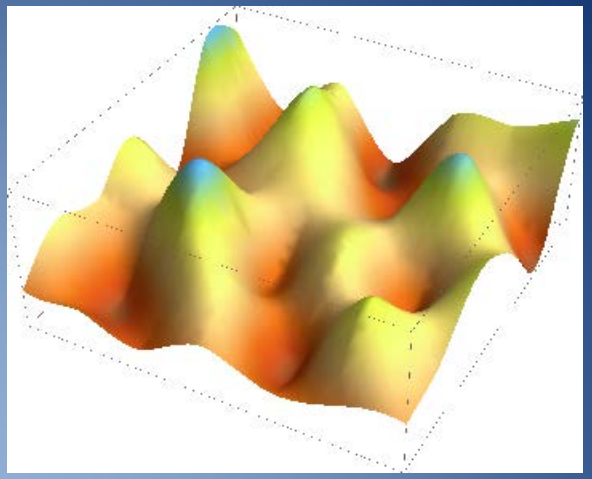

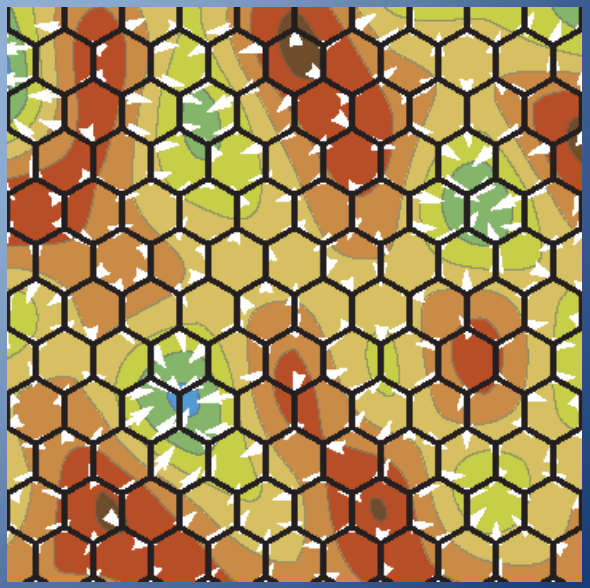

$$\vec{F}_{\vec{k}} = i\vec{k}V_{\vec{k}}$$

$$\vec{u}_{\vec{k}} = -\frac{\vec{F}_{\vec{k}}^{\parallel}}{(\lambda_L + 2\mu_L)\left|\vec{G} - \vec{k}\right|^2} - \frac{\vec{F}_{\vec{k}}^{\perp}}{\mu_L\left|\vec{G} - \vec{k}\right|^2}$$

$$\langle V_{\vec{k}}, V_{-\vec{k}} \rangle \simeq \bar{V}^2\xi^2\Big|_{|\vec{k}|\simeq G}$$

$$\frac{1}{\tau_s} \simeq \frac{\pi g_1^2 \bar{V}^2 \xi^2}{18(\lambda_L + 2\mu_L)^2 d_G^6 \alpha^4 \mathrm{v}_F k_F}$$

$$\frac{1}{\tau_g} \simeq \frac{16\pi g_2^2 \bar{V}^2 \xi^2}{9(\lambda_L + 2\mu_L)^2 d_G^6 \alpha^4 \mathrm{v}_F k_F} \left[\frac{1}{(\lambda_L + 2\mu_L)^2} + \frac{1}{\mu_L^2}\right]$$

$$\bar{n}^* \simeq \frac{32 g_1^2 \bar{V}^2 \xi^2}{9(\lambda_L + 2\mu_L)^2 \hbar^2 \mathrm{v}_F^2 d_G^6} \log\left(\frac{\Lambda}{k_F^*}\right)$$

$$\frac{1}{\mu \bar{n}^*} \simeq \frac{\hbar}{e} \frac{1}{4\log\left(\frac{\Lambda}{k_F^*}\right)} \left[\frac{1}{16\alpha^2} + \frac{g_2^2}{g_1^2}\left(1 + \frac{(\lambda_L + 2\mu_L)^2}{\mu_L^2}\right)\right]$$

$g_1 \approx 6.9$ eV

Bilayer graphene

$$H_g^{BLG} = \frac{t_\perp}{\hbar^2 v_F^2}\left[(k_x A_x - k_y A_y)\sigma_x + (k_x A_y + k_y A_x)\sigma_y\right]$$

$$\frac{1}{\tau_s^{BLG}} = \frac{4 v_F k_F}{t_\perp}\frac{1}{\tau_s^{SLG}}$$

$$\frac{1}{\tau_g^{BLG}} = \frac{2 v_F k_F}{t_\perp}\frac{1}{\tau_g^{SLG}}$$

$$\frac{1}{\mu_{BLG}} \simeq \frac{h}{e}\frac{k_F}{2\pi v_F}\left(\frac{4}{\tau_s^{SLG}} + \frac{2}{\tau_g^{SLG}}\right)$$

$$n^*_{BLG} = \frac{\sqrt{\langle V_s(\vec{r})^2\rangle}\, t_\perp}{\pi\hbar^2 v_F^2} \approx \frac{t_\perp}{\pi\hbar^2 v_F^2}\sqrt{\frac{32\pi g_1^2 \mu_L^2 \bar{A}}{9(\lambda_L + 2\mu_L)^2 d_G^6}}\log\left(\frac{\Lambda}{k_F^*}\right)$$

$$\frac{1}{\mu_{BLG}(\bar{n}^*_{BLG})^2} \simeq \frac{h}{e}\frac{\pi v_F^2}{2t_\perp^2 \log\left(\frac{\Lambda}{k_F^*}\right)}\left[\frac{1}{16\alpha^2} + \frac{g_2^2}{g_1^2}\left(1 + \frac{(\lambda_L + 2\mu_L)^2}{\mu_L^2}\right)\right] \simeq 920\frac{h}{e}\text{Å}^{-2}$$

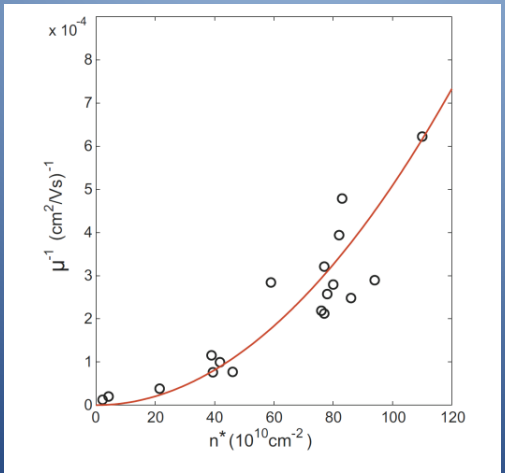

Raman measurements:
Correlations between strains and mobilities in graphene on BN

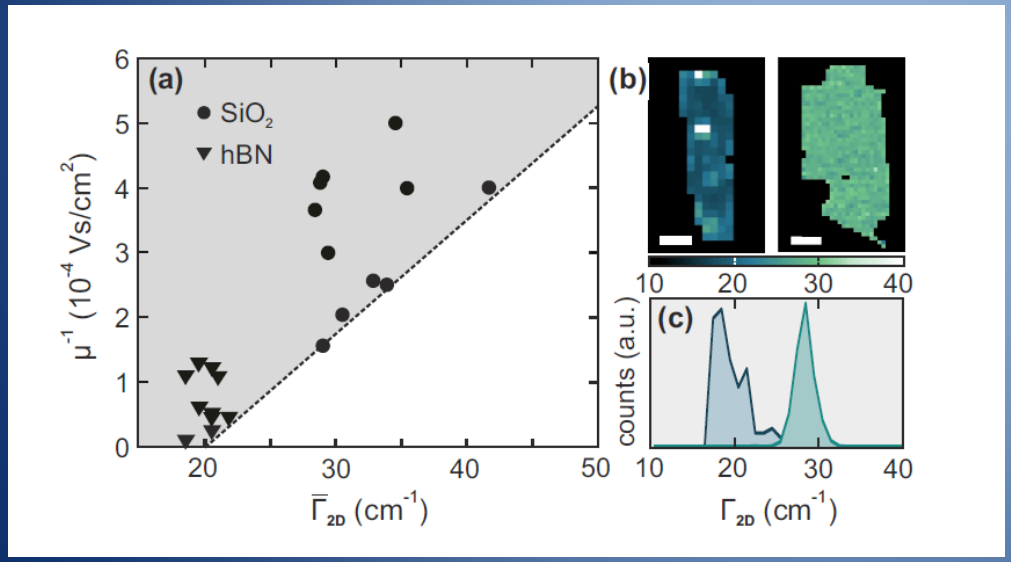

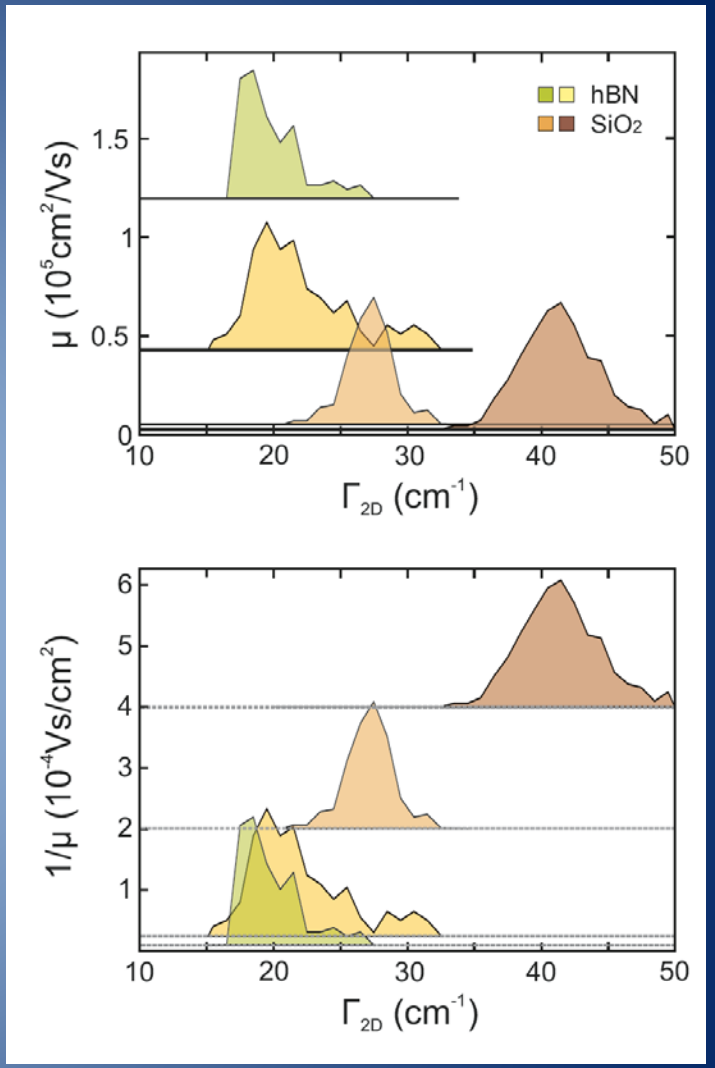

Anharmonic properties of graphene

- Anharmonic effects in membranes
- Negative thermal expansion coefficient
- Screening of the in plane stiffness
- The elastic response of graphene depends on the experimental setup (size, temperature, defects, pre existing strain, …)

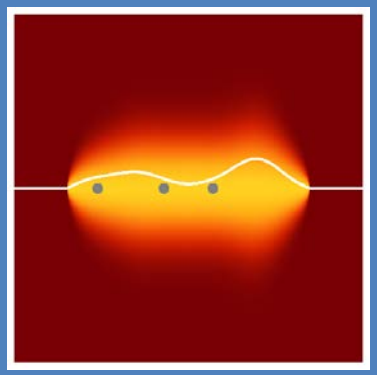

Stiffening graphene by controlled defect creation

Authors: Guillermo López-Polín[1], Cristina Gómez-Navarro[1,2*], Vincenzo Parente[3], Francisco Guinea[3], Mikhail I. Katsnelson[4], Francesc Pérez-Murano[5], and Julio Gómez-Herrero[1,2]

arXiv:1406.2131

Universal properties of transport in graphene

- Scattering is due to intravalley processes
- Interference processes (weak localization) are suppressed
- Puddles and transport are correlated
- Strains are the most likely origin of puddles and scattering

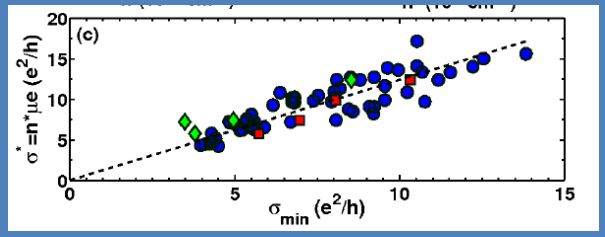

Random strain fluctuations as dominant disorder source for high-quality on-substrate graphene devices

Nuno J. G. Couto,[1] Davide Costanzo,[1] Stephan Engels,[2] Dong-Keun Ki,[1] Kenji Watanabe,[3] Takashi Taniguchi,[3] Christoph Stampfer,[4] Francisco Guinea,[5] and Alberto F. Morpurgo[1]

ArXiv:1401.5356,
Phys. Rev. X, in press

GOBIERNO DE ESPAÑA
MINISTERIO DE ECONOMÍA Y COMPETITIVIDAD

erc

GRAPHENE FLAGSHIP

Spinograph
Spintronics in Graphene

Spinograph
Spintronics in Graphene

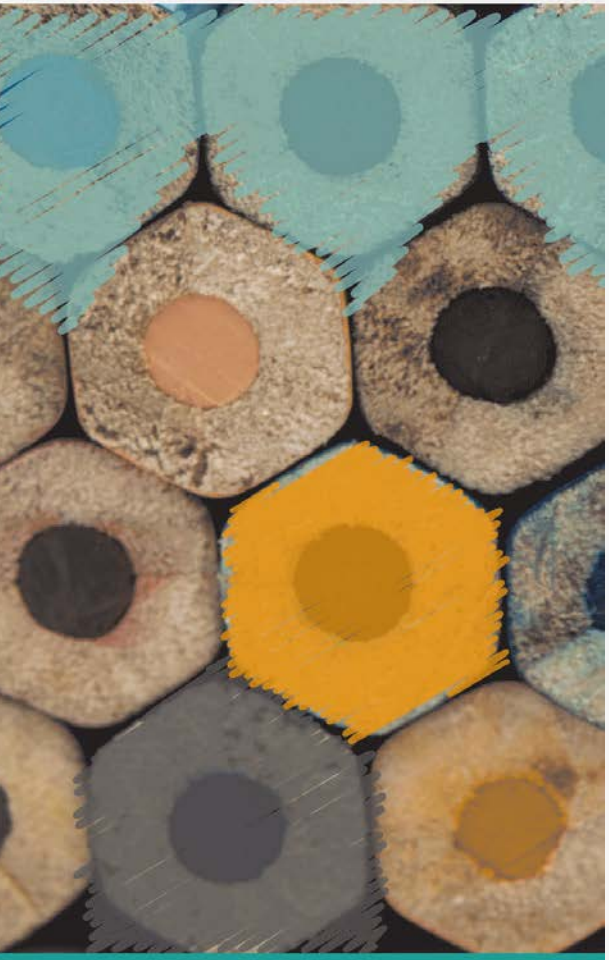

SPINOGRAPH is a *"Marie Curie Training Network Project (ITN)"*, funded by EU FP7

Spinograph
Spintronics in Graphene

ITN= Initial Training Network Marie Curie Program

TOPIC: Spintronics in graphene

Lifespan: Sep. 2013 – Aug 2017

Groups:

- 9 partners (CSIC; CNRS, Manchester, Groningen, Aachen, INL, Nanogune, Graphenea, AMO)
- 3 associated partners

#Trainees: 11 Phd students, 4 postdocs

Coordinated by

INL
INTERNATIONAL IBERIAN NANOTECHNOLOGY LABORATORY

MARIE CURIE ACTIONS